Holography in frequency-selective media. III. Spectral synthesis of arbitrary time-domain pulse shapes

Heinrich Schwoerer, Daniel Erni, and Alexander Rebane

Physical Chemistry Laboratory, Swiss Federal Institute of Technology, ETH-Zentrum, CH-8092 Zurich, Switzerland

Received May 13, 1994; revised manuscript received January 10, 1995

We study theoretically and experimentally the synthesis of arbitrary time-domain pulse shapes, using short laser pulses scattered by holograms stored in a spectrally selective hole-burning material. In general, writing holograms in spectrally selective materials results in cross talk and interference between different frequencies because of Kramers–Kronig dispersion relations. We discuss different ways to exclude the cross talk that disturbs faithful reproduction of the desired time-domain pulse shapes. In particular, we show that one can exclude the cross talk by writing holograms in a way that simulates a time-domain offset of the object pulse. To confirm our theoretical considerations we carry out experiments by writing persistent spectral hole-burning holograms with a tunable dye laser in an organic dye–polymer system at low temperature. By reading out the time-domain response with subpicosecond white-light pulses we demonstrate the feasibility of spectral synthesis of light pulses with complicated amplitude and phase properties on the time scale of hundreds of picoseconds with a subpicosecond time resolution.

Key words: spectrally selective data storage, holography, ultrashort pulses.

1. INTRODUCTION

Persistent spectral hole burning[1] (SHB) has produced numerous applications ranging from high-resolution spectroscopy of impurity centers in solids to new methods of frequency-selective optical data storage and processing.[2–4] The spectral selectivity of SHB is based primarily on the fact that at liquid-helium temperature the homogeneous absorption spectrum of a chromophore (organic dye molecule, rare-earth ion, color center, etc.) in a solid comprises a narrow, purely electronic zero-phonon line (ZPL), which typically has a width Γ_{ZPL} of $10^{-2}-10^{-4}$ cm^{-1} or less.[5] The second important contributing factor is the inhomogeneous broadening of the spectra because of the statistical distribution of the ZPL frequency associated with the inherent imperfection of the matrix structure. Persistent SHB occurs when, as a consequence of resonant irradiation in the inhomogeneously broadened band, the chromophores undergo tautomerization, ionization, or any other kind of structural change that shifts or radically alters the ZPL spectrum. Transient hole-burning mechanisms are also known, and they involve, in the case of rare-earth ions in crystals, accumulation of population in the hyperfine levels of the electronic ground state or, in the case of organic molecules, accumulation in the triplet state. As a result, the concentration of the chromophores that are absorbing resonantly at a given frequency decreases, and a narrow dip or hole is created in the inhomogeneous absorption spectrum.

From the point of view of holographic storage and coherent optical data processing, SHB offers a unique chance to alter, by illumination with light and with high spectral selectivity, the linear optical absorption coefficient of the media. At low temperatures the inhomogeneous width Γ_{inh} of the spectra often exceeds the homogeneous ZPL linewidth Γ_{ZPL} by a factor of 10^4 or more, allowing for a large multiplication factor in the frequency dimension. It has been demonstrated that, by means of a tunable cw monochromatic laser, holographic gratings can be recorded and detected as narrow spectral holes[6] leading to frequency-multiplexed storage and processing of holographic images.[4,7] In holographic hole burning the narrowest frequency interval required for storage of one hologram is given approximately by the value of Γ_{ZPL}, whereas the ratio $\Gamma_{inh}/\Gamma_{ZPL}$ of the inhomogeneous bandwidth over the homogeneous linewidth limits the ultimate number of independently addressable frequencies. It should be noted, however, that in general a spectrally narrow hologram diffracts light not only in the frequency interval of the burned hole but also to some extent at other frequencies outside this interval.[8] This happens, of course, because of the far-reaching wings of the frequency-domain refractive-index variation that, according to Kramers–Kronig dispersion relations, accompanies each narrow spectral hole in the index of absorption.

An alternative approach to writing spectrally selective holograms is to use a series of short pulses with a broad spectrum, which interfere with one another within the spectrally selective material.[9–13] The result of the interference between a temporally structured object pulse and a short δ-like reference pulse is a fringe pattern, in the frequency and the space dimensions, which is bleached in the absorption of the spectrally selective media. The stored information is retrieved by application of a short read pulse that stimulates a time-domain coherent recall (echo) that is either a direct or a time-inverted replica of the object pulse, depending on the time order of the pulses during the writing procedure. The longest possible duration of a time-domain signal recorded in this way is given by the homogeneous dephasing time, $\Delta t_{max} \sim T_2 = 1/2\pi\Gamma_{ZPL}$, whereas the inverse value of the inho-

0740-3224/95/061083-11$06.00

mogeneous bandwidth gives the shortest duration of the echo, $\Delta t_{\min} \sim 1/\Gamma_{\text{inh}}$.

The basic idea of time-domain holograms can be illustrated by the well-known principle of spatial Fourier holography, where, instead of taking the object itself, the hologram records the Fourier image of the object amplitude. During the readout the diffracted signal undergoes an inverse Fourier transformation, which then reproduces the replica of the object. In time-domain holography the spectrally selective material itself acts as a recorder of the Fourier spectrum of the object pulse. The inverse Fourier transformation back to the time dimension is performed by the echo amplitude stimulated by the read pulse. From this point of view, the time-domain hologram is equivalent to a collection of different narrow-band holograms, with each one corresponding to a certain monochromatic component of the object wave packet.[12]

In frequency-domain holography as well as in time-domain holography the read process is linear with respect to the amplitude of the read beam, whereas the writing process is also approximately linear with respect to the spectral intensity of the illuminating light. This means that the diffraction properties should not depend on the origin (cw or pulsed) of the hologram. Therefore it should be possible to use a cw monochromatic laser to write holograms in the frequency domain and then, by application of a short read pulse, it should be possible to produce any desired amplitude profile in time domain.

Spectral synthesis of arbitrary time-domain pulse shapes with spectrally nonselective materials was demonstrated in Refs. 14 and 15 by dispersion of the spectrum of a short light pulse in space with a diffraction grating and by use of a spatial modulator or a hologram to modify the relative amplitudes and phases of the frequency components. Another grating was then used to recombine the spatially separated frequencies into one time-modulated beam.

The time responses of spectrally programmed SHB transmission filters were studied in several papers.[11,16,17] According to elementary Fourier transformation, to implement the spectral synthesis of arbitrary pulse amplitudes in the time domain we also have to add to the spectral filtering the control over the phases of the spectral components. In the research reported in Ref. 18 narrow-band holograms with fixed relative phases were stored in a dye–polymer film at low temperature and were then illuminated with a subpicosecond spectral continuum to produce trains of short pulses in the diffracted beam.

There is, however, the principal problem of how to eliminate the interference between holograms at different frequencies. Because of the dispersion relations the diffraction also occurs, in general, outside the frequency interval of the burned absorption hole or hologram. If cross talk is present between different spectral components of the synthesized hologram, then the diffracted amplitude will not faithfully reproduce the desired time profile.

In our previous papers[19–21] we studied the cross talk between spectrally adjacent narrow-band holograms and showed that it is possible to reduce the interference if the phase of the hologram is recorded as a linear function of the frequency. We also showed that in the time domain the cross talk is connected to the principle of causality and is related to the diffraction asymmetry of thin, spectrally selective holograms with respect to the positive and the negative diffraction orders. In previous research it was also demonstrated that specially chosen frequency-dependent phase and amplitude functions bring about an improvement in the diffraction efficiency,[20,21] along with a better readout stability of cw holograms.[22]

Our first task in this paper is to formulate the sufficient conditions in which cross talk does not occur between spectrally nonoverlapping, but otherwise arbitrary, SHB holograms. For this purpose we express the amplitude and intensity distributions of the scattered light in the far diffraction zone behind a thin, spectrally selective hologram, illuminated with coherent monochromatic light, if the absorption comprises arbitrary structures. We proceed by considering the no-interference condition for two spectrally nonoverlapping grating structures and then generalize the result to an arbitrary hologram in the frequency dimension. This allows us to specify the sufficient condition for spectral synthesis of arbitrary time-domain pulse shapes.

In the second part of this paper we perform pulse synthesis experiments, using an organic dye–polymer photochemical hole-burning system at liquid-helium temperature. The purpose of the experiments is to verify some of our theoretical conclusions and to prove the feasibility of the spectral synthesis of complicated time profiles.

2. THEORY

A. Coherent Linear Response of Spectrally Selective Material

Consider a parallel plate of thickness l and transverse dimensions, $2a \times 2b$, made of a spectrally selective material with an inhomogeneously broadened absorption band of width Γ_{inh} (Fig. 1). Each small volume of the material is characterized by a certain frequency-domain structure of the inhomogeneous band. The absorption band itself is considered to be confined to a finite frequency interval $\{\nu_{\min}, \nu_{\max}\}$. At any frequency outside this interval the absorption of the plate is zero. The narrowest possible features in the absorption spectrum are limited by the homogeneous linewidth Γ_{ZPL}.

Let a linearly polarized monochromatic wave of frequency $\nu_{\min} < \nu_0 < \nu_{\max}$, propagating in the positive z-axis direction, illuminate the input surface of the plate in the x–y plane, as shown in Fig. 1. Here we consider only such optical responses that are linear with respect to the amplitude of the illuminating light. To exclude nonlinear effects, we always assume that the field amplitude of the incident light is less than

$$|E^{\text{in}}(t)| \ll \frac{h\Gamma_{\text{ZPL}}}{|\mathbf{d}|}, \tag{1}$$

where $\mathbf{d}$ is the dipole moment of the electronic transition and h is Planck's constant. Inequality (1) guarantees that the homogeneous linewidth is always much broader than any resonant Rabi frequency associated with the illuminating amplitude.[23]

Let us assume that the finest transverse spatial details of the absorption of the plate are much longer than l and

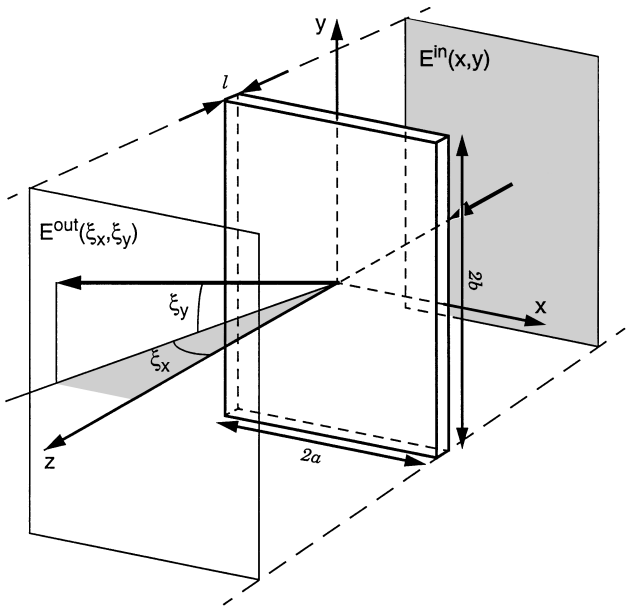

Fig. 1. Geometry of the readout of a spectrally selective hologram. The SHB material is a parallel plate of thickness l positioned in the x–y plane. The illuminating wave propagates in the positive direction of the z axis. The amplitude behind the hologram plate is characterized by two diffraction angles, ξ_x and ξ_y.

that the absorption is independent of the polarization of the light. Then the spectrally and the spatially selective intensity transmission of the plate can be described by a real function:

$$T(\nu, x, y) = \begin{cases} 0 < T(\nu, x, y) \le 1 & \text{if } |x| \le a, |y| \le b \quad \text{and} \quad \nu_{\min} \le \nu \le \nu_{\max} \\ 1 & \text{if } |x| \le a, |x| \le b \quad \text{and} \quad \nu_{\min} > \nu \quad \text{or} \quad \nu > \nu_{\max} \\ 0 & \text{otherwise} \end{cases} . \quad (2)$$

If we neglect the reflection by the surfaces of the plate, then this transmission function is directly related to the linear absorption coefficient of the material:

$$\alpha(\nu, x, y) = -\frac{\ln[T(\nu, x, y)]}{l} . \quad (3)$$

The absorption coefficient is given by the convolution of the ZPL-frequency inhomogeneous distribution function $g(\nu)$, with the homogeneous line-shape function $\gamma(\nu)$ (Ref. 2):

$$\alpha(\nu) = \int_0^\infty g(\nu')\gamma(\nu - \nu')\mathrm{d}\nu' . \quad (4)$$

The information about the SHB medium in the frequency domain is stored not in the transmission but rather in the inhomogeneous distribution function, and the coherent response of the plate also depends on the phonon sideband, along with any other structure accompanying the ZPL. Here, for simplicity, we consider only the ZPL and ignore all the other features of the homogeneous spectra.

In general, calculating the coherent optical response of the resonant media requires solving coupled Maxwell–Bloch equations for the amplitude of the light wave traveling through the plate. Here we assume that the amplitude is varying in the z direction slowly compared with the wavelength and that the variation in time of the amplitude envelope is also slow, which means that the electric-field strength of the light beam obeys the first-order wave equation. Under the weak-excitation condition (1), the equation describing the polarization of the resonant media is linear as well and can be solved trivially, together with the wave equation.[12,17,24] Then the relation between the amplitude of the monochromatic wave directly before the plate and the transmitted wave amplitude directly after the plate, $E^{\mathrm{out}}(x, y)$, can be expressed through a simple formula:

$$E^{\mathrm{out}}(x, y)\exp(i2\pi\nu_0 t) = K(\nu_0, x, y) \cdot E^{\mathrm{in}}(x, y)[\exp\{i2\pi\nu_0[t - (l/c)]\}] , \quad (5)$$

where c is speed of light and $K(\nu, x, y)$ is the complex amplitude response function:

$$K(\nu, x, y) = [T(\nu, x, y)]^{1/2}\exp(i\hat{H}\{\ln[T(\nu, x, y)]^{1/2}\}) , \quad (6)$$

with the Hilbert transformation being defined according to

$$\hat{H}[f(\nu)] = \frac{1}{\pi}\int_{-\infty}^{\infty} \frac{f(\nu')}{\nu' - \nu}\mathrm{d}\nu' . \quad (7)$$

Although formula (6) is suitable for direct numerical calculations, evaluation of an analytic expression requires further simplifications. For this purpose we note that the absorption coefficient can be written as a sum of two functions:

$$\alpha(\nu, x, y) = \alpha_0(\nu) - \Delta\alpha(\nu, x, y) , \quad (8)$$

where $\Delta\alpha(\nu, x, y)$ is the variation of the absorption coefficient that is due to SHB and α_0 is the absorption before the bleaching. If $\Delta\alpha(\nu, x, y)l \ll 1$, then we can develop the exponential function given in Eq. (6) into a series and retain only the first two terms, which leads to

$$K(\nu, x, y) = K_0 + \kappa(1 + i\hat{H})[\Delta\alpha(\nu, x, y)] , \quad (9)$$

where κ is a constant and K_0 is the response function before SHB.

In actual experiments the signals are monitored not directly after the plate but rather at some distance behind it. If the free wave propagation distance L is large compared with the transverse dimensions of the plate, then the observed amplitude can be expressed as

$$E^{\mathrm{out}}(\xi_x, \xi_y) = \frac{\nu_0}{cL}\int_{-a}^{a}\int_{-b}^{b} E^{\mathrm{in}}(x, y)K(\nu_0, x, y) \times \exp\left[-i\frac{2\pi\nu_0}{c}(x \sin \xi_x + y \sin \xi_y)\right]\mathrm{d}x\mathrm{d}y , \quad (10)$$

where ξ_x and ξ_y are the angles of diffraction in the x and the y directions, respectively (see Fig. 1).

Let us now accept the following assumptions: (a) the illuminating monochromatic beam is a plane wave with

unit amplitude; (b) the spatial structure of the plate depends only on the x coordinate; (c) the amplitude response of the plate is given by formula (9). Then the angular distribution of the light intensity in the far diffraction region is proportional to

$$I^{\mathrm{out}}(\xi_x) \propto |K_0|^2 \frac{\sin\left(\frac{2\pi a\nu_0 \sin\xi_x}{c}\right)^2}{\left(\frac{\pi\nu_0 \sin\xi_x}{c}\right)^2} + \kappa^2 \left| \int_{-a}^{a} (1 + i\hat{H})[\Delta\alpha(\nu, x)] \times \exp\left[-i\frac{2\pi\nu_0}{c} x \sin\xi_x\right] \mathrm{d}x \right|^2 + 2\,\mathrm{Re}\left\{ \kappa K_0 \frac{\sin\left(\frac{2\pi a\nu_0 \sin\xi_x}{c}\right)}{\left(\frac{\pi\nu_0 \sin\xi_x}{c}\right)} \times \int_{-a}^{a} (1 + i\hat{H})[\Delta\alpha(\nu, x)] \times \exp\left(-i\frac{2\pi\nu_0}{c} x \sin\xi_x\right) \mathrm{d}x \right\}. \quad (11)$$

The first term in the above equation describes the prompt response of the plate without any structure, the second term is the intensity scattered from the SHB structure, and the third term describes interference between the prompt response and the scattered light. If the diffraction angle of the scattered signal is larger than the angular distribution of the prompt response, then the interference term vanishes. Below we keep only the second term and drop the other two. We also set the integration limits equal to infinity, which means that we neglect the diffraction on the edges of the hologram plate.

We can see from relation (11) that, because the Hilbert transformation involves the integral over all frequencies, the signal intensity at the read frequency ν_0 depends, in general, on the structure recorded at all other frequencies between $\nu_{\min}$ and $\nu_{\max}$, even if Γ_{ZPL} is small.

B. Cross Talk between Two Spectrally Nonoverlapping Holograms

Consider two interfering coherent laser beams writing holograms in the absorption spectrum of the SHB plate. Let the recorded structure consist of two gratings:

$$\Delta\alpha(\nu, x) = s_1(\nu, x)\{1 + \cos[2\pi(x/\Lambda_1) + \phi_1(\nu, x)]\} + s_2(\nu, x)\{1 + \cos[2\pi(x/\Lambda_2) + \phi_2(\nu, x)]\}, \quad (12)$$

where $\Lambda_{1,2}$, $s_{1,2}$, and $\phi_{1,2}$ are the spatial period, the amplitude envelope, and the phase of the grating, respectively. Our assumption is that the two holograms are recorded at different frequencies in such a way that the envelope functions have no overlap in the frequency dimension:

$$s_1(\nu, x)s_2(\nu, x) = 0. \quad (13)$$

After substituting Eq. (12) into Eq. (10), we find that the amplitude in the far diffraction zone consists of a zeroth-order term and first-order diffraction terms. The total diffracted amplitude from the first and the second gratings is

$$E^{(\pm 1)}(\xi_x) \propto \int (1 + i\hat{H})\{s_1(\nu, x)\exp[\pm i\phi_1(\nu, x)]\} \times \exp\left[-i\frac{2\pi\nu_0 x}{c}\left(\sin\xi \mp \frac{c}{\nu_0\Lambda_1}\right)\right]\mathrm{d}x + \int (1 + i\hat{H})\{s_2(\nu, x)\exp[\pm i\phi_2(\nu, x)]\} \times \exp\left[-i\frac{2\pi\nu_0 x}{c}\left(\sin\xi \mp \frac{c}{\nu_0\Lambda_2}\right)\right]\mathrm{d}x. \quad (14)$$

We call the terms with a plus (minus) the phase factor the $+1$ (-1) diffraction order. If we now explicitly calculate the intensity [relation (11)], we can see that there are interference terms between two holograms. Here, for simplicity, we write only one of these terms (the others are similar):

$$I^{(\mathrm{interf})}(\xi_x) \propto \left(\int \{s_1(\nu_0, x)\exp[\pm i\phi_1(\nu_0, x)]\} \times \exp\left[-i\frac{2\pi\nu_0 x}{c}\left(\sin\xi \mp \frac{c}{\nu_0\Lambda_1}\right)\right]\mathrm{d}x \right)^* \times \int \hat{H}\{s_2(\nu, x')\exp[\pm i\phi_2(\nu, x')]\} \times \exp\left[-i\frac{2\pi\nu_0 x'}{c}\left(\sin\xi \mp \frac{c}{\nu_0\Lambda_2}\right)\right]\mathrm{d}x'. \quad (15)$$

The magnitude of $I^{(\mathrm{interf})}$ characterizes the amount of cross talk between the two holograms. We say that the cross talk is minimal when all the interference terms are minimal or are equal to zero.

One case in which cross talk does not occur is when the spatial period of the two gratings is different ($\Lambda_1 \neq \Lambda_2$). The integration over the x coordinate in relation (15) then yields two different diffraction angles, $\xi_{1,2} = \pm a\,\sin(c/\nu_0\Lambda_{1,2})$. This means that at a sufficiently large distance behind the plate the two diffracted waves will separate, and no interference takes place.

Let us assume now that both gratings have the same spatial period ($\Lambda_1 = \Lambda_2$). This allows us to rewrite relation (15) as

$$I^{(\mathrm{interf})}(\xi_x) \propto \int \left(\int \{s_1(\nu_0, x + x')\exp[\pm i\phi_1(\nu_0, x + x')]\}^* \times \hat{H}\{s_2(\nu, x')\exp[\pm i\phi_2(\nu, x')]\}\,\mathrm{d}x' \right) \times \exp\left[-i\frac{2\pi\nu_0 x'}{c}(\sin\xi \pm \sin\xi_1)\right]\mathrm{d}x. \quad (16)$$

We can see that the integral over the spatial coordinate inside the boldface parentheses is proportional to the cross correlation of the two spatial envelope functions. If the two functions are largely different, then the cross-correlation integral is small, and the cross talk will also

not occur. Such a situation is encountered, for example, if SHB holograms are recorded by means of an object beam scattered from a random screen or diffuser.[25]

Below we assume that the holograms are written with plane waves, so that there is no specific structure associated with the spatial envelopes of the holograms. In this case the integration over the spatial variable is trivial, and expression (16) simplifies to

$$I^{(\text{interf})}(\xi_x) \propto (\{s_1(\nu_0)\exp[\pm i\phi_1(\nu_0)]\})^* \times \hat{H}\{s_2(\nu)\exp[\pm i\phi_2(\nu)]\}\delta(\xi + \xi). \quad (17)$$

We now show how to make expression (17) vanish. For this purpose we recall the property of the Hilbert transformation[26] that states that when the transformation is applied to the product of two functions, one of which is changing slowly compared with the other, the slowly varying function can be removed outside the Hilbert transform symbol. For example, when $0 < \Omega < \omega_0$, then

$$\hat{H}(\cos\ \Omega t\ \cos\ \omega_0 t) = \hat{H}(\cos\ \omega_0 t)\cos\ \Omega t. \quad (18)$$

If the narrowest features in the frequency envelope of the holograms are all large compared with the homogeneous linewidth, then we can always choose the phase function $\phi(\nu)$ such that

$$\hat{H}\{s(\nu)\exp[i\phi(\nu)]\} = \hat{H}\{\exp[i\phi(\nu)]\}s(\nu). \quad (19)$$

In other words, if the phase is changing faster than the amplitude envelope function, then the spectral envelope of the hologram can be removed outside the Hilbert transform symbol. If we now insert Eq. (19) into relation (17), then, because of the nonoverlap condition (13), the cross talk is exactly zero:

$$I^{(\text{interf})}(\xi_x) \propto [s_1(\nu_0)s_2(\nu_0)]\exp[\mp i\phi_1(\nu_0)] \times \hat{H}\{\exp[\pm i\phi_2(\nu)]\}\delta(\xi + \xi_1) = 0. \quad (20)$$

This means that Eq. (19) expresses a sufficient condition for making the cross talk between two spectrally nonoverlapping holograms disappear.

There are, of course, many different phase functions that can satisfy Eq. (19). The simplest choice is a linear function, $\phi(\nu) = \varepsilon - 2\pi\nu\tau$, where τ is the inverse oscillation period and ε is an arbitrary constant. In this case

$$\hat{H}[\exp(i\varepsilon - i2\pi\nu\tau)] = \begin{cases} -i\ \exp(i\varepsilon - i2\pi\nu\tau) & \text{if } \tau > 0 \\ i\ \exp(i\varepsilon - i2\pi\nu\tau) & \text{if } \tau < 0 \end{cases}. \quad (21)$$

It should be noted that, so far, we have not made any specific assumptions about the interval separating the two holograms in the frequency. This means that, as long as our assumptions (13) and (19) are valid, the two holograms can be as close to each other as necessary, including the limit of zero frequency separation.

If the SHB plate contains many spectrally nonoverlapping holograms, then it is straightforward to generalize the above result to this case as well: when each hologram satisfies condition (19), the cross talk vanishes for each pair of holograms and therefore also for the whole spectral structure.

C. Spectral Synthesis of Arbitrary Time-Domain Pulses

Let the plate be illuminated with a bandwidth-limited laser pulse of such short duration that its spectrum is constant over the whole width of the inhomogeneous absorption band. We require that the diffraction in the +1 order reproduce a given temporal pulse shape of amplitude $S_p(t)\exp(i2\pi\nu_0 t)$. Here ν_0 is the carrier frequency coinciding with the center of the inhomogeneous absorption band. Time zero of the complex envelope $S_p(t)$ corresponds approximately to the center of the desired pulse. The shortest duration of the desired signal is not less than the time resolution of the material $\Delta t_{\min}$, and the longest duration is not more than $\Delta t_{\max}$.

We can always write a set on N spectrally nonoverlapping gratings in such a way that the total spectral amplitude of the hologram structure is proportional to the modulus of the spectral amplitude of the desired function:

$$\sum_{j=1}^{N} S_j(\nu) \propto |S_p(\nu)| = \left| \int_{-\infty}^{\infty} S_p(t')\exp[-i2\pi(\nu - \nu_0)t']\mathrm{d}t' \right|. \quad (22)$$

We choose the phases of the holograms in such a way that, on the one hand, the phase of the diffracted light reproduces the phase of the desired function and, on the other hand, there is no cross talk between any two of the N holograms. The latter is accomplished as soon as we attribute to each of the holograms a phase function satisfying condition (19). The time response amplitude is then given by inverse Fourier transformation:

$$E^{(\pm 1)}(t) = \int \left(\sum_{j=1}^{N} s_j(\nu')(1 + i\hat{H})\{\exp[\pm i\phi_j(\nu')]\} \right) \times \exp(i\nu' t)\mathrm{d}\nu'\delta(\xi \mp \xi_1). \quad (23)$$

It follows from relation (22) that, to avoid additional modulation of the spectrum, the Hilbert transform of the phase function has to give a function with unit modulus—the condition satisfied by the linear function $\phi_j(\nu) = \varepsilon_j - 2\pi\nu\tau_j$. Now we can choose the constants ε_j such that the phase of the diffracted light follows the phase of the spectral components of the desired function. The last step that we take is to set all factors equal, $\tau_j = \tau_{\max} > 0$. After we take Eq. (21) into account, the diffracted amplitude in the +1 order is proportional to the desired function with the time delay τ:

$$E^{(1)}(t) = \int \left[\sum_{j=1}^{N} s_j(\nu')2\exp(i\varepsilon_j) \right] \times \exp[i\nu'(t - \tau)]\mathrm{d}\nu' \propto S_p(t - \tau). \quad (24)$$

At the same time, the amplitude in the −1 order is zero:

$$E^{(-1)}(t) = 0. \quad (25)$$

We pointed out in Section 1 that in the limit of weak excitation the diffraction properties of spectral gratings recorded with narrow-band light are closely related to those recorded with spectrally broad pulses. In this sense formulas (24) and (25) reproduce the result known as the phase-matching condition for stimulated photon

echo.[27] By choosing the phase function of spectrally synthesized holograms one can make the diffracted signal appear preferentially in either the positive or the negative diffraction order.

To gain more insight into the physical meaning of the phase function, let us consider what will happen if relation (22) is valid but condition (19) is not fulfilled. For example, if we set $\tau = 0$, then the time response is

$$E^{(1)}(t) \propto S_p(t)\Theta(t)$$
$$E^{(-1)}(t) \propto S_p(-t)\Theta(t), \tag{26}$$

where $\Theta(t)$ is the unit step function:

$$\Theta(t) = \begin{cases} 1 & \text{if } t \geq 0 \\ 0 & \text{if } t < 0 \end{cases}. \tag{27}$$

From here we can see that, if the time offset is zero (or smaller than the duration of the desired signal at the negative times), then in the +1 diffraction order only a part of the desired pulse will appear. The remaining part of the time profile will be diffracted in the −1 order and will occur inverted in time.

If we again draw a parallel between frequency-domain and time-domain recording of spectrally selective holograms, then we can say that formulas (26) describe the direct and the time-inverted amplitudes of stimulated photon echo.[9,11] This statement clarifies the meaning of condition (19): to exclude the cross talk between any number of spectrally nonoverlapping holograms, it is sufficient to store each hologram in such a way that there is a time offset between the object and the reference beams at least as large as the duration of the coherent time response.

We can now formulate the condition for the Fourier synthesis as follows: faithful reproduction in the +1 diffraction order is achieved if there is a positive time offset between the reference and the object beams that is larger than the duration of the negative part of the desired time profile. This time offset can be either real or simulated by a linear phase function; in both cases the scattering occurs only in the +1 order. In the opposite case, if the time offset is too short, then one part of the amplitude will be cut off, will appear in the opposite diffraction order, and will be inverted in time.

It is interesting that in this time-domain formulation our conditions formally coincide with what is required for writing time-domain holograms.[9–12] There the nonoverlap in time of the reference and the object pulses automatically guarantees that condition (19) is satisfied. Therefore it is not surprising that, in experiments on time-domain storage, usually no cross talk occurs between different spectral components.

3. EXPERIMENTAL DETAILS

The SHB storage medium that we use is a 100-μm-thick poly(vinyl butyral) film doped at a concentration of 10^{-3} mol/L with chlorin (2,3-dihydroporphyrin) molecules. During the experiments the sample is contained at 2 K in a ^{4}He bath cryostat with pass-through optical windows. At low temperature the $S_1 \leftarrow S_0$ absorption band of chlorin peaks at 634 nm; at this wavelength the optical density of our sample (before hole burning) is 2.5. The inhomogeneous bandwidth of chlorin (FWHM) is 150 cm^{-1}, and the homogeneous linewidth has a value of $\Gamma_{ZPL} = 5.4 \times 10^{-3}$ cm^{-1} at 1.7 K.[28]

The part of the setup that is used to write the holograms is schematically shown in Fig. 2(a). To burn the persistent spectral holes we use a conventional synchronously pumped picosecond dye laser. A 50% beam splitter divides the output beam of the dye laser into a reference beam and an object beam. After reflecting back from plane mirrors the beams again pass through the same beam splitter, but at a slightly different angle, so that they can be picked up by two separate mirrors. The two beams are then brought to overlap on the SHB sample inside the cryostat at an angle of $\xi = 5°$. The optical

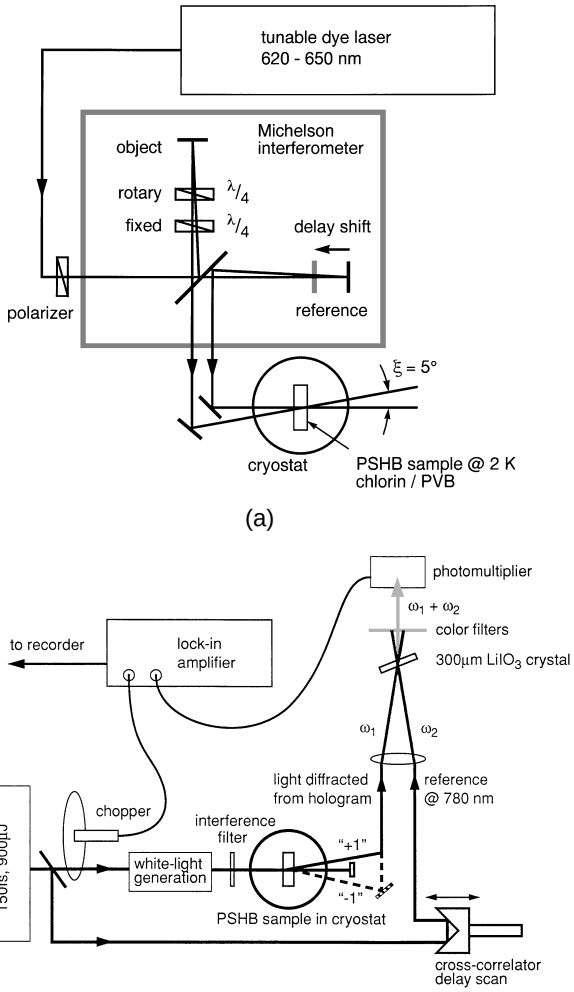

Fig. 2. (a) Scheme for writing SHB holograms. The dye laser beam is split into reference and the object beams and is recombined at the sample positioned in an optical ^{4}He bath cryostat. The delay of the object pulse with respect to the reference pulse is variable from 0 to 100 ps. One controls the phase between the object and the reference beams by rotating the second quarter-wave plate (see text). (b) Experimental setup to measure the time response of the holograms. A small fraction of the Ti:sapphire fundamental pulse is split off by a glass plate and is used as a reference in the cross correlator. The rest is focused into a block of quartz glass to generate a white-light continuum. The interference filter has a spectral window of 250 cm^{-1} centered at 635 nm. PVB, poly(vinyl butyral); PSHB, persistent SHB.

path length of the reference arm of the interferometer can be changed by movement of the mirror, which varies the delay between the object and the reference beams at the sample position in an interval of 0–100 ps.

To control the phase between the two writing beams, we use a technique based on the phase shift associated with cyclic changes of the state of polarization of light (Pancharatanam phase).[29] For this purpose we insert into the object arm of the interferometer two zero-order quarter-wave plates. The first wave plate is adjusted at an angle of 45° with respect to the vertical polarization direction of the incoming laser beam. The second quarter-wave plate is mounted upon a rotating stage driven by a motor. At the output of the interferometer the object beam always has the same linear polarization as the input beam, independent of the rotation angle of the second wave plate. The phase of the object beam changes in proportion to the rotation angle of the second quarter-wave plate, $\phi = 2\theta$. In our experiments it is important that the rotation of the wave plate not change the optical path length of the object beam. This allows us to set two quantities, the time offset and the phase, independent of each other. In addition, this device provides an arbitrarily large continuous phase shift without influencing the delay between the reference and the object beams.

The size of the illuminated spot of the sample is 2 mm in diameter, and the combined average intensity of the writing beams is approximately 1 mW. The diffraction efficiency by the SHB holograms produced after an exposure time of approximately 100 s is of the order of 1%.

Figure 2(b) shows the principle of the time-domain readout of the holograms. The readout is carried out by use of 200-fs-duration pulses at the wavelength of the chlorin absorption band. One obtains these pulses by focusing the 780-nm output (pulse duration, 150 fs; pulse energy, 0.9 mJ) of a 1-kHz-repetition-rate amplified Ti:sapphire laser (Clark MXR) in a block of quartz glass. The laser light is partially converted into a white-light continuum by self-phase modulation in the glass. The white-light beam is collimated and is directed through a bandpass interference filter that cuts out a spectral interval of 250 cm^{-1} overlapping the inhomogeneous absorption band of chlorin. The light scattered from the hologram in either the +1 or the −1 diffraction direction is picked up by a mirror and is then focused, together with the fundamental Ti:sapphire laser pulses, in a 300-μm-thick $LiIO_3$ crystal. A lock-in technique involving a mechanical chopper is used to record the intensity at the sum frequency between the Ti:sapphire laser and the light scattered from the hologram as a function of the delay in the cross correlator.

4. DISCUSSION OF EXPERIMENTAL RESULTS

In Ref. 18 it was demonstrated that SHB holograms recorded with a narrow-band laser can select arbitrary frequency components out of the broad spectrum of a femtosecond continuum pulse. Our first experiment in this study is designed to demonstrate that the spectral components can be obtained with variable predefined relative phases. As a simple example, we recorded, one after the other, two holograms near the maximum of the inhomogeneous absorption band by illuminating the sample with the reference and the object beams of spectral width $\Delta\nu = 0.5$ cm^{-1}. In this experiment the delay of the object beam with respect to the reference beam is 30 ps. Before making the second exposure, we change the frequency of the dye laser by $\Delta\nu = 7.3$ cm^{-1} and rotate the wave plate by a given angle θ. After the writing is completed, we block the dye laser beam and illuminate the sample in the direction of the reference beam with 250-cm^{-1}-broad femtosecond continuum. The light scattered from the hologram in the +1 diffraction directions is then cross correlated with the Ti:sapphire laser pulses in the nonlinear crystal.

Figure 3 presents the cross-correlation signal intensity as a function of the delay between the Ti:sapphire laser pulse and the scattered light. The time envelope of the scattered light has a duration of approximately 80 ps, which roughly corresponds to the inverse value of the spectral width of each of the two holograms. The signal contains a coherent beat with a period equal to the inverse value of the frequency interval between the holograms, $(\Delta\nu\, c)^{-1} = 4.7$ ps. If we compare traces (a)–(e), obtained at different wave-plate rotation angles θ, then we can see that the positions of the beat maxima and minima in time are moving in proportion to the rotation angle of the wave plate. This result verifies that we are indeed able to control the relative phase between the holograms.

The dashed curve in Fig. 3(e) shows the results of numeric modeling of the time-domain response of the hologram in the +1 order based on formula (6). Almost perfect correspondence of the theory to the experiment is achieved, especially because formula (6) takes into account not only the shape of the hologram grating but also the inhomogeneous band shape of the sample, its opti-

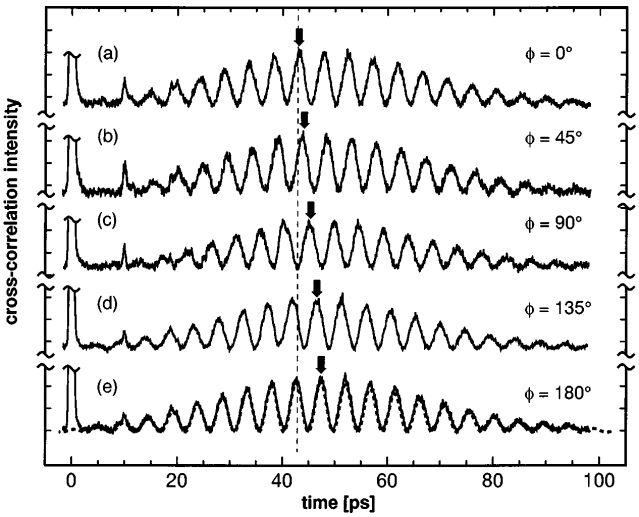

Fig. 3. Dependence on the delay of the cross-correlation intensity of the signal diffracted in the +1 order. The SHB plate contains two adjacent holograms stored with a frequency interval of 7.3 cm^{-1}. (a)–(e) Different cross-correlation traces corresponding to writing holograms with different relative phases (ϕ = 0°, 45°, 90°, 135°, 180°) set by rotation of the second quarter-wave plate. The peak at the zero delay in the experimental traces is an artifact that occurs because of residual scattering of the readout pulse on the sample surfaces and in the bulk of our sample.

cal density, and the contrast of the hologram. To illustrate this point further, Fig. 4 shows part of the structure of the inhomogeneous band of the sample corresponding to Fig. 3 in the frequency and the spatial dimensions. The contour plot in Fig. 4 shows an expanded view of the fringe pattern of one of the two holograms.

In Section 2 we showed that, to achieve a faithful reproduction of the desired time profile, there must be a large enough time offset programmed into the object amplitude. If this condition is fulfilled, then the scattering occurs in only one diffraction order, and the time profile of the scattered light is given by the Fourier transform of the written-in frequency-domain pattern. If the time offset chosen is too short, then one part of the amplitude will be cut off and will appear in the opposite diffraction order. In the experiment described in Subsection 2.C, one produces the amplitude profile $s(\nu)$ by changing the laser frequency over a broad interval of $15\,700-15\,850$ cm^{-1}, which covers most of the inhomogeneous absorption band of chlorin molecules. The phase function $\varepsilon(\nu)$ is produced by synchronous rotation of the wave plate with the frequency of the illuminating laser. One sets the time delay by moving the mirror in the reference arm of the interferometer.

Figure 5 shows the result of the cross correlation of the diffracted light with the fundamental laser pulse when the holograms are recorded with a fixed time offset of 15 ps and a constant phase function. The time-domain responses of two holograms with essentially different frequency-dimension amplitude profiles are compared. In the first case one records the hologram by continuously scanning the dye laser frequency with a constant speed over the 150-cm^{-1} range. The average exposure at each frequency is then nearly constant, and no sharp features are burned into the amplitude profile of the hologram. Condition (19) is then well satisfied, and the diffracted signal appears in only one +1 order [Fig. 5(a)]. Figures 5(b) and 5(c) show how the time response changes if the spectral profile contains sharp features. In this case the hologram is created by illumination of the SHB sample with a 0.5-cm^{-1}-wide laser line at 16 different fixed frequencies placed at equal intervals of 7.3 cm^{-1}. A direct Fourier transform of such spectral structure would be a periodic train of sharp pulses under a 50-ps-broad, nearly Gaussian envelope. Because the holes are now relatively narrow, condition (19) is only partially fulfilled, and the signal appears in both the positive [Fig. 5(b)] and the negative [Fig. 5(c)] diffraction directions. We can also see that the signal in the −1 order contains the complementary, but time-inverted, part of the +1-order signal.

To compare our results with earlier time-domain experiments, we note that in the case of photon echoes correlation occurs between echo shapes and the shape of the particular excitation pulse[10–12,30,31] and that time inversion is observed if a certain temporal ordering of the excitation pulses is used. In our case the holograms are recorded with a cw light, and the temporal ordering exists only virtually, in the sense of a given phase function; however, because of the linearity of the response, during the readout the hologram behaves as if there were a real time delay.

In Fig. 6 we show that our considerations are also valid if we write the holograms by modulating only the phase of the object beam. We record the holograms by continuously scanning the dye laser frequency with a constant speed over the 150-cm^{-1} range in the same way as in the experiment of Fig. 5(a), but during the frequency scan the wave plate is also rotated. Figure 6(a) essentially repeats what is shown in Fig. 5(a), whereas both the phase and the amplitude functions are constant, with the exception that the time offset has a different value

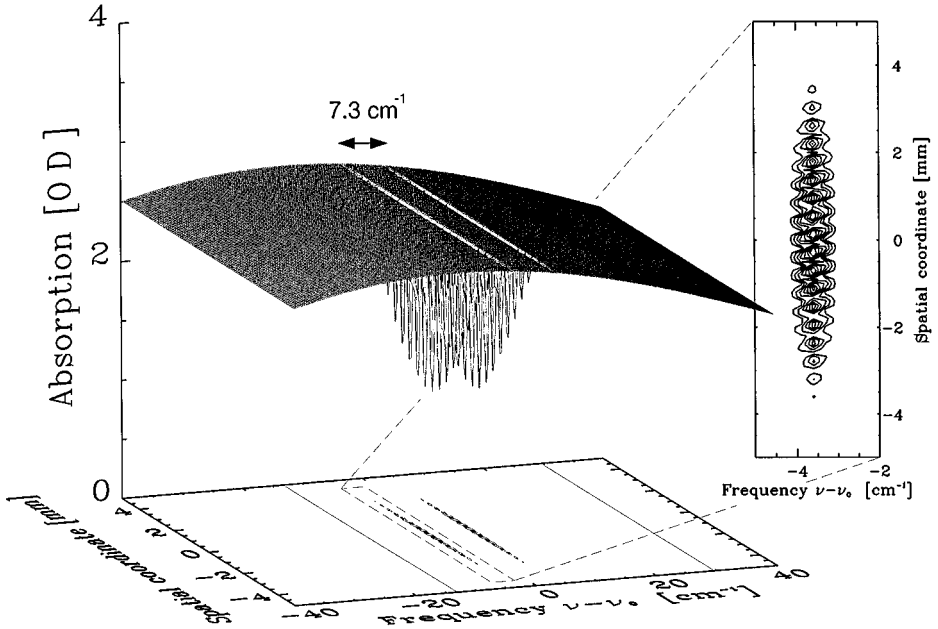

Fig. 4. Simulation of the frequency- and the spatial-domain structure of the hologram corresponding to the time-domain signal shown in Fig. 3. (The angle between the object and the reference beams is chosen to be smaller than in the experiment only for better visualization.) The theoretical (dashed) curve shown in Fig. 3 is obtained when the transmission function shown here is substituted into formula (10). OD, optical density.

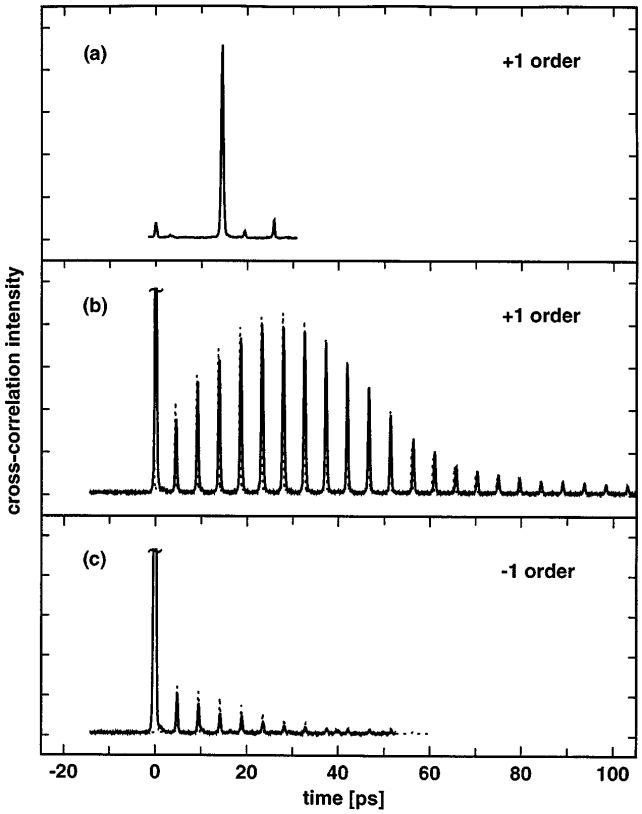

Fig. 5. Cross correlation of the fundamental pulse with the hologram signal with fixed time offset (15 ps) and constant phase but different intensity profiles in the frequency dimension. (a) The hole profile is constant in the 15 700–15 850-cm^{-1} interval. The diffracted signal appears only in the +1 order. (b), (c) The profile consists of 16 narrow holes burned at a constant interval of 7.3 cm^{-1}. The signal appears in both (b) the positive and (c) the negative diffraction directions. The dashed curve is the simulated time-domain intensity obtained by Fourier transform of the frequency-domain amplitude profile.

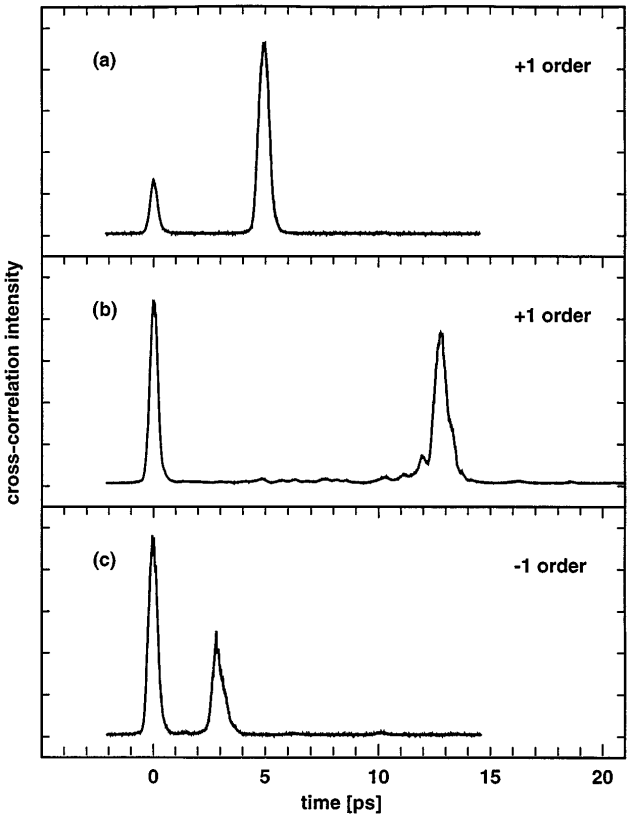

Fig. 6. Cross correlation of the fundamental pulse with the hologram signal with fixed time offset 5 ps and constant intensity in the 15 700–15 850-cm^{-1} frequency interval but different phase function profiles in the frequency dimension. (a) The phase is constant. The diffracted signal appears only in the +1 order. (b) The phase function is $\varepsilon(\nu) = 0.45\pi$ cm^{-1}. The signal appears only in the +1 order. (c) The phase function is $\varepsilon(\nu) = -0.45\pi$ cm^{-1}. The signal appears only in the −1 order.

of 5 ps. In Fig. 6(b) the hologram is recorded while the wave plate is rotated in the positive direction according to $\varepsilon(\nu) = 0.45\pi/\mathrm{cm}^{-1}$. The Fourier transform of this phase function corresponds to an additional time delay of +8 ps. This means that the modulation of the phase of the hologram is faster than the additional linear phase function built in by the 5-ps time offset. However, because the signs of the phase factors are both positive, the result is an even larger delay, so that condition (19) is not violated. As expected, the hologram signal appears in the +1 order and at a time delay of 13 ps. The situation changes if the wave plate is rotated in the negative direction, where $\varepsilon(\nu) = -0.45\pi/\mathrm{cm}^{-1}$ [Fig. 6(c)]. Then the two phase factors have different signs, and, instead of the sum, the difference of the two values is obtained. The result is a total negative time offset, and the signal appears only in the −1 order, with a delay of 3 ps.

In the following examples we demonstrate that one achieves Fourier synthesis of rather complicated pulse sequences by writing holograms with given phase and amplitude functions. Figure 7(a) shows the pulse train that is produced when the intensity profile consists of 16 narrow holes burned, one after the other, at a constant interval of 7.3 cm^{-1}. For each fourth exposure the wave plate was rotated by $\theta = 90°$, which changes the

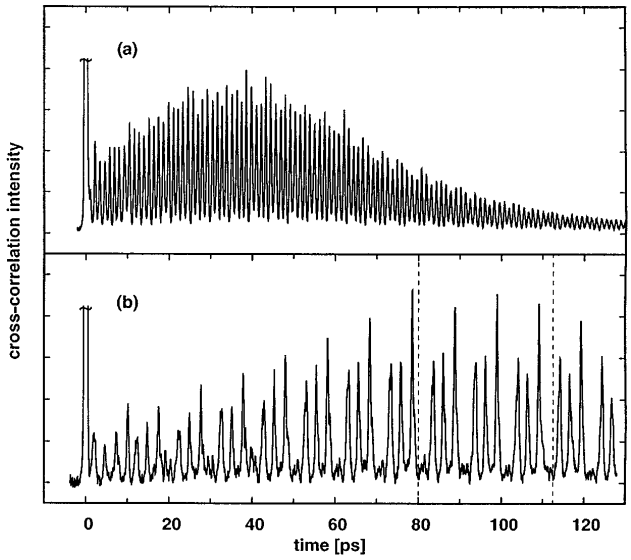

Fig. 7. Synthesis of pulse trains in the +1 diffraction direction with different amplitude and phase functions in frequency dimension. (a) The intensity profile consists of 16 narrow holes burned at a constant interval of 7.3 cm^{-1}. The phase function changes by π for each fourth hole. (b) The intensity profile is the same as in (a), but the phase function changes according to a more complicated function (see text).

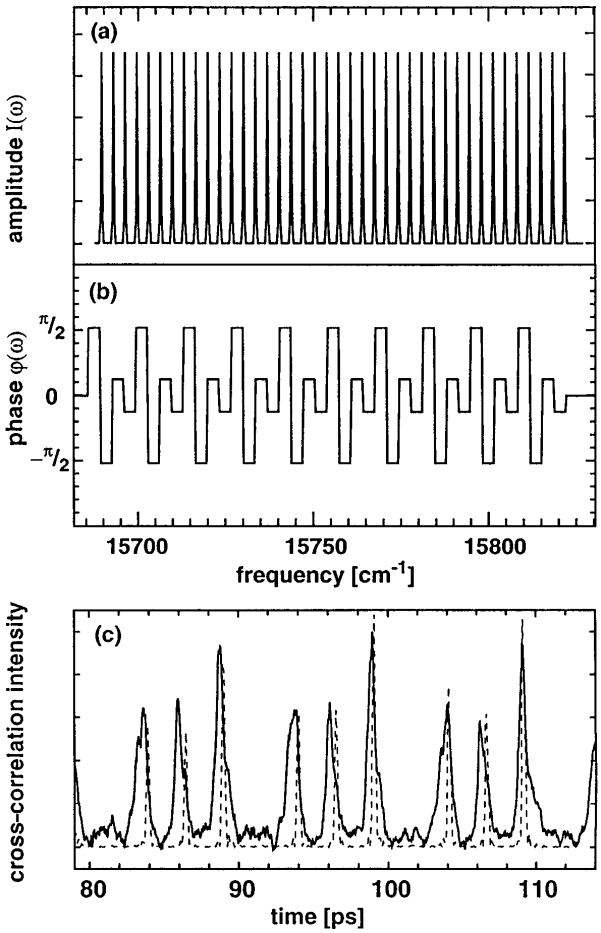

Fig. 8. Theoretical (a) amplitude and (b) phase functions used to generate the pulse sequence shown in Fig. 7(b). (c) Part of the experimental cross-correlation trace (solid curve) shown in comparison with the theoretically calculated time-domain intensity function (dashed curve).

phase by π. Fourier transform of such an amplitude and phase function yields a pulse train with a period of 1.2 ps. Figure 7(a) shows that this is exactly what can be observed in the experiment. Of course, so as not to lose much signal to the -1 diffraction order, we chose a sufficiently large time delay. Figure 7(b) shows another periodic pulse train that can be observed when the intensity profile is written in the same way as in Fig. 7(a) but the phase changes according to a more complicated function. Figure 8 shows the amplitude and the phase functions that we use in this case, along with the details of the experimental cross-correlation trace in comparison with the theoretically calculated time-domain hologram response.

It should be noted that the experiment reproduces exactly what is expected from the theory. It may be of practical interest that, on the one hand, the time resolution that we achieve is better than 1 ps, which corresponds to terahertz modulation in the time domain. On the other hand, in our experiment the duration of the pulse trains exceeds 100 ps, which means that by this method it is possible to generate programmed trains of several hundreds of pulses.

5. CONCLUSIONS

We have presented theoretical and experimental evidence that spectral programming of time-domain pulse shapes in a spectrally selective hole-burning material is feasible with high temporal resolution. In contrast, we have also theoretically analyzed how to eliminate cross talk between spectrally nonoverlapping holograms. Two different approaches can be taken. The first is to write holograms so that they have different scattering angles or noncorrelating spatial structures. The second, more general way to suppress the interference is to modulate the phase of the holograms in the frequency dimension. Our theoretical analysis also reveals aspects of the inherent connection between spectrally selective hologram storage and the principle of causality.

ACKNOWLEDGMENTS

We thank Urs P. Wild for valuable discussions about this paper. This research was supported by the Swiss Priority Program of Optical Sciences, Applications, and Technologies.

REFERENCES

1. A. A. Gorokhovskii, R. K. Kaarli, and L. A. Rebane, "Hole burning in the contour of a pure electronic line in a Shpolskii system," JETP Lett. **20,** 216–219 (1974); B. M. Kharlamov, R. I. Personov, and L. A. Bykovskaya, "Stable gap in absorption spectra of solid solutions of organic molecules by laser irradiation," Opt. Commun. **12,** 191–194 (1974).
2. L. A. Rebane, A. A. Gorokhovskii, and J. V. Kikas, "Low-temperature spectroscopy of organic molecules in solids by photochemical hole burning," Appl. Phys. B **29,** 235–250 (1982); J. Friedrich and D. Haarer, "Photochemical hole burning: spectroscopic study of relaxation processes in polymers and glasses," Angew. Chem. Int. Ed. Engl. **23,** 113–140 (1984).
3. W. E. Moerner, ed., *Persistent Spectral Hole Burning: Science and Applications*, Vol. 44 of Topics in Current Physics (Springer-Verlag, Berlin, 1988), and references therein.
4. K. Holliday and U. P. Wild, "Spectral hole burning," in *Molecular Luminescence Spectroscopy. Part 3*, S. G. Schulman, ed., Vol. 77 of Chemical Analysis Series (Wiley, New York, 1993), p. 149.
5. K. K. Rebane, *Impurity Spectra of Solids* (Plenum, New York, 1970).
6. A. Renn, A. J. Meixner, U. P. Wild, and F. A. Burkhalter, "Holographic detection of photochemical holes," Chem. Phys. **93,** 157–162 (1985).
7. A. Renn and U. P. Wild, "Spectral hole burning and hologram storage," Appl. Opt. **26,** 4040–4042 (1987); A. J. Meixner, A. Renn, and U. P. Wild, "Spectral hole burning and holography. I. Transmission and holographic detection of spectral holes," J. Chem. Phys. **91,** 6728–6736 (1989); U. P. Wild, A. Renn. C. De Caro, and S. Bernet, "Spectral hole burning and molecular computing," Appl. Opt. **29,** 4329–4331 (1990).
8. A. Renn, A. J. Meixner, and U. P. Wild, "Spectral hole burning and holography. II. Diffraction properties of two spectrally adjacent holgorams," J. Chem. Phys. **92,** 2748–2755 (1990).
9. T. W. Mossberg, "Time-domain frequency-selective optical data storage," Opt. Lett. **7,** 77–79 (1982).
10. N. W. Carlson, L. J. Rothberg, A. G. Yodh, W. R. Babbitt, and T. W. Mossberg, "Storage and time reversal of light pulses using photon echoes," Opt. Lett. **8,** 483–485 (1983).
11. A. K. Rebane, R. K. Kaarli, and P. M. Saari, "Hole burning by coherent sequences of picosecond pulses," JETP Lett. **38,**

383–386 (1983); A. Rebane, R. Kaarli, P. Saari, A. Anijalg, and K. Timpmann, "Photochemical time-domain holography of weak picosecond pulses," Opt. Commun. **47,** 173–176 (1983); A. Rebane and R. Kaarli, "Picosecond pulse shaping by photochemical time domain holography," Chem. Phys. Lett. **101,** 317–319 (1983).
12. P. Saari and A. Rebane, "Time- and space-domain holography of pulsed light fields in a spectrally photo-active medium," Proc. Estonian Acad. Sci. Phys. Math. **33,** 322–332 (1984); P. Saari, R. Kaarli, and A. Rebane, "Picosecond time- and space-domain holography by photochemical hole burning," J. Opt. Soc. Am. B **3,** 527–533 (1986); A. Rebane, "Coherent recall and time–space holography in impurity systems with photochemical hole-burning," Ph.D. dissertation (Institute of Physics, Estonian Academy of Sciences, Tartu, Estonia, 1985).
13. A. Rebane, J. Aaviksoo, and J. Kuhl, "Storage and time reversal of femtosecond light signals via persistent spectral hole burning holography," Appl. Phys. Lett. **54,** 93–95 (1989); A. Rebane and J. Feinberg, "Time-resolved holography," Nature **351,** 378–380 (1991); H. Gygax, A. Rebane, and U. P. Wild, "Stark effect in dye-doped polymers studied by photochemically accumulated photon echo," J. Opt. Soc. Am. B **10,** 1149–1158 (1993).
14. Yu. T. Mazurenko, "Holography of wave packets," Appl. Phys. B **50,** 101–114 (1990).
15. A. M. Weiner, D. E. Leaird, D. H. Reitze, and E. G. Paek, "Femtosecond spectral holography," IEEE J. Quantum Electron. **28,** 2251–2261 (1992).
16. M. Mitsunaga, R. Yano, and N. Uesugi, "Spectrally programmed stimulated photon echo," Opt. Lett. **16,** 264–266 (1991).
17. H. Sõnajalg, A. Gorokhovskii, R. Kaarli, V. Palm, M. Rätsep, and P. Saari, "Optical pulse shaping by filters based on spectral hole burning," Opt. Commun. **71,** 377–380 (1989).
18. H. Schwoerer, D. Erni, A. Rebane, and U. P. Wild, "Subpicosecond pulse shaping via spectral hole burning," Opt. Commun. **107,** 123–128 (1994).
19. A. Rebane, S. Bernet, A. Renn, and U. P. Wild, "Holography in frequency selective media: hologram phase and causality," Opt. Commun. **86,** 7–13 (1991).
20. S. Bernet, B. Kohler, A. Rebane, A. Renn, and U. P. Wild, "Holography in frequency selective media. II. Controlling the diffraction efficiency," J. Lumin. **53,** 215–218 (1992).
21. S. Bernet, B. Kohler, A. Rebane, A. Renn, and U. P. Wild, "Spectral hole burning and holography. V. Asymmetric diffraction from thin holograms," J. Opt. Soc. Am. B **9,** 987–991 (1992).
22. S. Bernet, "Phasenkontrollierte Holographie in frequenzselektiven Materialien," Ph.D. dissertation Diss ETH Nr. 10292 (Swiss Federal Institute of Technology, Zurich, 1993).
23. L. Allen and J. H. Eberly, *Optical Resonance and Two-Level Atoms* (Wiley, New York, 1975).
24. J. H. Eberly, S. R. Hartmann, and A. Szabo, "Propagation narrowing in the transmission of a light pulse through a spectral hole," Phys. Rev. A **23,** 2502–2506 (1981); M. D. Crisp, "Propagation of small-area pulses of coherent light through a resonant medium," Phys. Rev. A **1,** 1604–1611 (1970).
25. A. Rebane, "Associative space-and-time domain recall of picosecond light signals via photochemical hole burning holography," Opt. Commun. **65,** 175–178 (1988); "Associative recall of time- and space-domain holograms in spectrally selective photo-active medium," Proc. Estonian Acad. Sci. Phys. Math. **37,** 89–92 (1988).
26. D. E. Vakman and L. A. Vainstein, "Amplitude, phase, frequency—fundamental concepts of oscillation theory," Sov. Phys. Usp. **20,** 1002–1016 (1977).
27. T. W. Mossberg, R. Kachru, and S. R. Hartmann, "Echoes in gaseous media: a generalized theory of rephasing phenomena," Phys. Rev. A **20,** 1976–1996 (1979).
28. A. J. Meixner, A. Renn, S. E. Bucher, and U. P. Wild, "Spectral hole burning in glasses and polymer films: the Stark effect," J. Phys. Chem. **90,** 6777–6785 (1986).
29. T. H. Chyba, L. J. Wang, L. Mandel, and R. Simon, "Measurement of the Pancharatnam phase for a light beam," Opt. Lett. **13,** 562–564 (1988).
30. S. O. Elyutin, S. M. Zakharov, and E. M. Manykin, "Theory of formation of photon echo pulses," Sov. Phys. JETP **49,** 421–431 (1979).
31. V. A. Zuikov, V. V. Samartsev, and R. G. Usmanov, "Correlation of the shape of photon echo signals with the shape of excitation pulses," JETP Lett. **32,** 270–274 (1980).